# Spectroscopically Probing Microscopic Solvent Properties of Room-Temperature Ionic Liquids with the Addition of Carbon Dioxide

**Jie Lu,[†,‡] Charles L. Liotta,[§,‡] and Charles A. Eckert*[,†,‡]**

*Schools of Chemical Engineering and Chemistry and Biochemistry, and Specialty Separations Center, Georgia Institute of Technology, Atlanta, Georgia 30332-0100*

*Received: November 22, 2002; In Final Form: February 20, 2003*

Room-temperature ionic liquids (RTILs) provide an alternative for elimination of solvent emissions to the atmosphere for many reactions, but the subsequent separation of the products by conventional methods can be a challenge. However, the use of supercritical carbon dioxide ($scCO_2$) as an extractant offers potential for a novel class of environmentally benign media for chemical reaction and downstream separation. We have investigated the solvent properties of mixtures of 1-butyl-3-methyl imidazolium hexafluorophosphate ([bmim][$PF_6$]) and $CO_2$ as functions of temperature (35−50 °C) and $CO_2$ pressure (0−230 bar). We report the Kamlet−Taft dipolarity/polarizability parameter, volume expansion, and microviscosity. The results are consistent with a picture of local enhancement of RTIL composition around a chromophore, maintaining solvent strength even at fairly high loadings of $CO_2$, whereas the microviscosity in the vicinity of the solute is dramatically reduced, leading to enhanced mass transport and facilitated separation.

## Introduction

Room-temperature ionic liquids (RTILs), organic salts composed entirely of cations and anions that remain liquid at or below room temperature, are potential green solvents for applications in synthesis,[1−4] biocatalysis,[5,6] electrochemistry,[7] and separation.[8] Recently developed RTILs consist of pyridinium or imidazolium cation coupled with an anionic counterpart, such as $PF_6^-$, $BF_4^-$, $N(SO_2CF_3)_2^-$, etc. Because RTILs have easily modified structures and properties, they are often called "designer solvents". Lack of effective vapor pressure is characteristic of RTILs, which offers opportunities not only for replacement of volatile organic solvents, but also for facilitation of certain separation processes, such as distillation. RTILs are nonflammable, and most exhibit high thermal stability.[9,10] They typically have an extensive liquid range up to 300 °C, which allows for substantial convenience in optimization of a multiple-step process that requires manipulating over a wide temperature range. More significantly, they can function as good solvents for a wide variety of ionic and organic compounds.

Supercritical carbon dioxide ($scCO_2$, $T_c = 31.1$ °C, $P_c = 73.8$ bar) is an environmentally benign medium that has undergone the most intensive investigation as an alternative to undesirable organic solvents in the past two decades.[11] $CO_2$ is a safe and inexpensive medium, and its physical properties can be continuously adjusted from gaslike to liquidlike by temperature and pressure. As a consequence of its low viscosity, mass transport is greatly enhanced in $scCO_2$ relative to that in liquids. In addition, $scCO_2$ offers facile solvent removal solely by depressurization.

Blanchard et al. have reported that several ionic liquids can uptake a considerable amount of $CO_2$, despite the negligible solubility of ionic liquids in the $CO_2$ phase.[12,13] This auspicious phase behavior of the RTIL/$CO_2$ system offers the opportunity for incorporating $CO_2$ with ionic liquids, as demonstrated in a number of applications.[8,14−20] First, downstream processing for product separation and catalyst recovery has become a challenge for the rapidly growing area of synthetic chemistry using RTILs. Current processes mainly include evaporation and liquid/liquid extraction, which can either be difficult, be detrimental to the product, or have undesirable environmental consequences. $ScCO_2$ has shown the potential as an effective medium for quantitatively extracting a wide variety of organic compounds from an RTIL phase with no loss of the solvent.[21] The significance of $CO_2$ extraction is highlighted by both the environmental advantages of $CO_2$ and complete elimination of the problem of cross-contamination encountered in liquid/liquid extraction.

Second, biphasic catalysis in RTIL/$scCO_2$ has drawn increasing attention.[15−18,22] In addition to improved selectivity and quantitative yield, a built-in advantage exists for facile separation and catalyst recovery by utilization of $CO_2$. As interesting as the potential applications, the fundamental knowledge of the solution structure of RTIL/$CO_2$ mixtures on a microscopic level has been the focus of several recent efforts.[23,24] Kazarian et al. studied Lewis acid−base interactions between $CO_2$ and anions of RTILs using an ATR−IR technique.[24] Baker and co-workers reported experimental results on microscopic solution properties such as Py-scale and viscosity.[23] In the current work, we measured the Kamlet−Taft $\pi^*$ parameter and the extent of volume expansion for mixtures of 1-butyl-3-methyl imidazolium hexafluorophosphate ([bmim][$PF_6$]) and $CO_2$ as functions of temperature and pressure based on the solvatochromic behavior of the indicator *N*,*N*-dimehthyl-4-nitroaniline. The effects of added $CO_2$ on the microviscosity and local dielectric property of [bmim][$PF_6$] were also evaluated using 9-(dicyanovinyl)-julolidine (DCVJ) as a fluorescence spectroscopic probe. Comparison of our results with a similar investigation by Baker

* Corresponding author. Tel.: 01-(404) 894-7070. Fax: 01-(404) 894-9085. E-mail: cae@che.gatech.edu.
† School of Chemical Engineering.
‡ Specialty Separations Center.
§ School of Chemistry and Biochemistry.

10.1021/jp0224719 CCC: $25.00 
Published on Web 04/15/2003

et al.[23] provides insight into solute-specific solvent effects and preferential solvation processes.

## Experimental Section

**Materials.** The RTIL [bmim][$PF_6$] was provided by SACHEM (purity of 97%). To eliminate possible moisture, [bmim][$PF_6$] was held under vacuum at ambient temperature for approximately 1 week prior to use. Carbon dioxide was a product from Matheson (SFC grade, 99.99% purity). The solvatochromic indicator *N,N*-dimethyl-4-nitroaniline (Aldrich, 97%) and the fluorescence probe DCVJ (Molecular Probes) were used as received. All organic solvents were of the highest purity available from Sigma-Aldrich and used without further purification.

**Apparatus.** A stainless steel vessel with three sapphire windows (6.4-mm-thick) was constructed for UV−vis and fluorescence spectroscopy. The windows were sealed with Teflon gaskets capable of withstanding pressures exceeding 250 bar. The path length of the cell is 2.2 cm, and the internal volume is 9.6 $cm^3$ at room temperature. The temperature control unit (Omega) for the cell consists of heating cartridges inserted into the body, a microprocessor thermometer, and a temperature controller. The temperature variation was maintained within ±0.1 °C of the setpoint. Pressure was monitored by a pressure transducer and a pressure readout (Druck) with an uncertainty of 0.01% in the range of 0−207 bar. A Teflon-coated spin bar constantly agitated the contents in the cell throughout measurements to facilitate equilibrium. The solvatochromic measurements and spectrum processing were performed on a Hewlett-Packard 8453 diode array UV−vis spectrophotometer (1-nm resolution and ±0.2-nm wavelength accuracy). A Shimadzu RF-5301PC spectrofluorophotometer provided all of the fluorescence spectra with ±1.5 nm wavelength accuracy.

**Procedure.** The dried [bmim][$PF_6$] solution with an indicator of an appropriate concentration was loaded into the high-pressure vessel and degassed under vacuum at a given temperature for at least 24 h prior to measurement. The solution visible through the optical windows was the RTIL phase. Initial spectroscopic measurements were conducted in the absence of $CO_2$, and then $CO_2$ was pressurized into the cell with a syringe pump (ISCO). Phase equilibrium was ensured by observation that the spectrum and pressure no longer changed with time (equilibration took longer to achieve at lower $CO_2$ pressures). $CO_2$ was added repeatedly until the highest pressure was reached at each temperature. Reproducibility was tested at continuously decreasing pressure for the same content by releasing $CO_2$ and conducting spectral measurements when each equilibrium was achieved. All the solvatochromic spectra were corrected by subtraction of the spectrum of the corresponding pure solvent. The initial concentrations of *N,N*-dimethyl-4-nitroaniline and DCVJ in [bmim][$PF_6$] without added $CO_2$ were $2.0 \times 10^{-5}$ and $4.5 \times 10^{-6}$ mol/L, respectively. The density of pure $CO_2$ was calculated by an equation of state.[25] The viscosity and dielectric constant for conventional liquids were obtained from the DIPPR 801 Thermophysical Properties Database (2002 Public Release).

## Results and Discussion

**I. Solvatochromic Behavior of *N,N*-Dimethyl-4-Nitroaniline.** *Kamlet−Taft Dipolarity/Polarizability Parameter (π*).* The π* parameter provides a comprehensive measure of the ability of a solvent to stabilize a solute molecule based on the dielectric effects.[26] It is a quantitative index of solvent dipolarity/polarizability that also provides insight into the local solvent environment surrounding an indicator molecule. The experimental determination of π* is classically based on the solvatochromism (solvent-induced spectral shift) of seven designated spectroscopic indicators, among which 4-nitroanisole and *N,N*-dimethyl-4-nitroaniline are the primary and secondary candidates, respectively. The latter, however, was chosen as the single indicator for measuring π* in this work because its solvatochromic peak is readily distinguishable from the UV−vis absorbance of [bmim][$PF_6$]. The solvatochromic absorbance of *N,N*-dimethyl-4-nitroaniline corresponding to the spectral band at the longest wavelength is attributed to the $\pi \rightarrow \pi^*$ electronic transition due to an intramolecular charge transfer from $N-(CH_3)_2$ (electron donor) to $NO_2$ (electron acceptor) through the aromatic system. Characteristically, the first excited state exhibits a higher polarity than the ground state. The dispersive, inductive, and electrostatic interactions between the indicator and a given solvent are therefore considered the primary contributors to the solvatochromic shift. Cyclohexane ($\pi^* = 0.00$) and dimethyl sulfoxide (DMSO, $\pi^* = 1.00$) were measured as the reference solvents for normalization of the π* scale. The quantitative calculation of π* value is given by

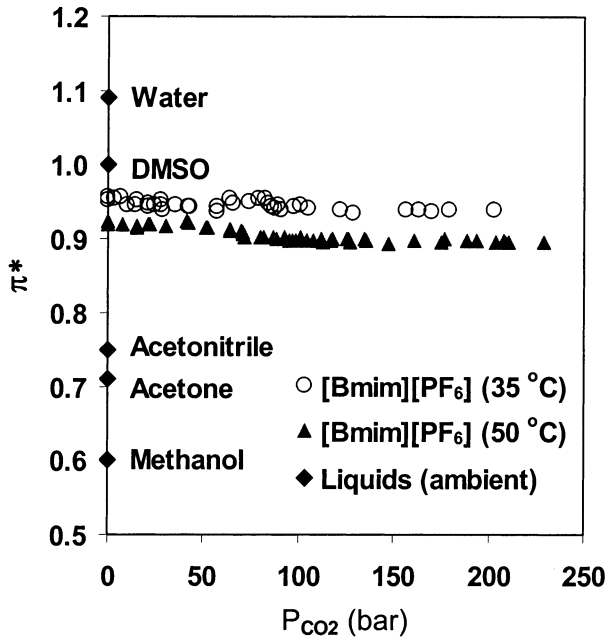


**Figure 1.** Kamlet−Taft π* parameter (dipolarity/polarizability) for conventional organic solvents and for [bmim][$PF_6$]/$CO_2$ as a function of $CO_2$ pressure.

$$\pi^* = \frac{[\nu(\mathrm{s}) - \nu(\mathrm{cyclohexane})]}{[\nu(\mathrm{DMSO}) - \nu(\mathrm{cyclohexane})]} \quad (1)$$

where ν is the frequency ($cm^{-1}$) of the solvatochromic peak maximum and s refers to the solvent under measurement.

Figure 1 displays π* parameters for [bmim][$PF_6$]/$CO_2$ mixtures as a function of $CO_2$ pressure at 35 and 50 °C. The dipolarity/polarizability of pure [bmim][$PF_6$] at 35 °C is higher than that at 50 °C and agrees with the previously published temperature dependence of π* for pure [bmim][$PF_6$].[27] With the addition of $CO_2$ to [bmim][$PF_6$], the π* parameter undergoes minimal reduction at a constant temperature. For example, π* changes from 0.95 for neat [bmim][$PF_6$] to only 0.94 for the mixture at 203 bar and 35 °C. Similarly, pure [bmim][$PF_6$] has a π* value of 0.92 that changes to 0.90 as the pressure increases to 230 bar at 50 °C. In comparison with conventional solvents, π* of [bmim][$PF_6$] both with and without $CO_2$ is slightly lower than those of water (1.09) and DMSO (1.0), but appreciably

higher than those of acetonitrile (0.75), acetone (0.71), and methanol (0.60).[28−31]

Blanchard et al. determined a $CO_2$ solubility of approximately 80 mol % in dried [bmim][$PF_6$] at a pressure of 100 bar and a temperature of 40 °C.[12] Preferential solvation between the RTIL and the indicator might be a reasonable interpretation for the insignificant effect of substantial amounts of $CO_2$ on the apparent polarity of [bmim][$PF_6$]. The molecular interaction between the RTIL of strong polarity and the polar solute appears to be dominant over the weak solute−$CO_2$ interaction, suggesting that the competitive RTIL−solute interaction might result in selective aggregation of [bmim][$PF_6$] around the indicator molecule. The solvent strength is preserved in a wide concentration range of $CO_2$ present because of the [bmim][$PF_6$]-enriched microenvironment. In practice, one may expect a limited effect of $CO_2$ on the solubility of organics in RTILs if the polar solute−solvent interaction plays a key role in the dissolution process. On the other hand, Baker and co-workers reported a decline in the value of $I_1/I_3$ (another polarity scale) for fluorescent pyrene (nonpolar) in [bmim][$PF_6$]/$CO_2$ as the pressure of $CO_2$ increases.[23] The existence of a solute-specific solvent effect in RTIL/$CO_2$ systems could account for the discrepancy between the two studies.

*Volume Expansion of [Bmim][$PF_6$] by Added $CO_2$.* Solvatochromic spectra can also be used to estimate the extent of volume expansion of [bmim][$PF_6$] by added $CO_2$ based on two assumptions about the spectral analysis. The first assumption is that the amount of *N*,*N*-dimethyl-4-nitroaniline partitioning into the $CO_2$ fluid phase is negligible. This assumption was justified experimentally, because the absorbance intensities of the indicator are reproducible in pure ionic liquid before the addition as well as after the release of $CO_2$—this would not occur if the $CO_2$ phase stripped the indicator. Second, we assume that the extinction coefficient of the solvatochromic peak for the indicator remains constant in neat [bmim][$PF_6$] and in the [bmim][$PF_6$]/$CO_2$ mixtures investigated.

The expansion factor in this context is defined as the ratio of the volume of the mixture ($V_m$) to that of neat [bmim][$PF_6$] ($V_0$) at a constant temperature. The expression $V_m/V_0 = A_0/A_m$ can be inferred from the Lambert−Beer law, where $A$ denotes the intensity of the solvatochromic peak in the corresponding solution. The expansion factor of the [bmim][$PF_6$] phase as a function of $CO_2$ pressure at 35 and 50 °C is displayed in Figure 2. The extent of volume expansion is greater at 35 °C than 50 °C at the same pressure. The two arrows in Figure 2 indicate the pressure where the density of the $CO_2$ phase becomes identical to the critical density ($\rho_c = 10.6$ mol/L for pure $CO_2$) at the two different temperatures. The expansion factor appears to undergo a sharp increase at lower pressures and then to level off as the density of $CO_2$ in the vapor phase approaches the critical density. At 35 °C, for instance, the volume of [bmim][$PF_6$] can be expanded by adding $CO_2$ to levels of 33 and 42% at 78 and 200 bar, respectively.

**II. Fluorescent Molecular Rotor.** The high viscosity of [bmim][$PF_6$] and many other RTILs could be a limitation for practical applications by potentially hindering mass-transfer-limited reaction or decreasing separation efficiency. Fortunately, $CO_2$ acts as an effective diluent to reduce the viscosity and, therefore, promote mass transfer in the viscous RTILs. We investigated the influence of $CO_2$ on the local viscosity of [bmim][$PF_6$] to better understand the role $CO_2$ plays in tuning transport properties of RTILs on the molecular level. The fluorescence probe DCVJ (see Figure 3) is well-described as a solvent-dependent molecular rotor that is characterized by a

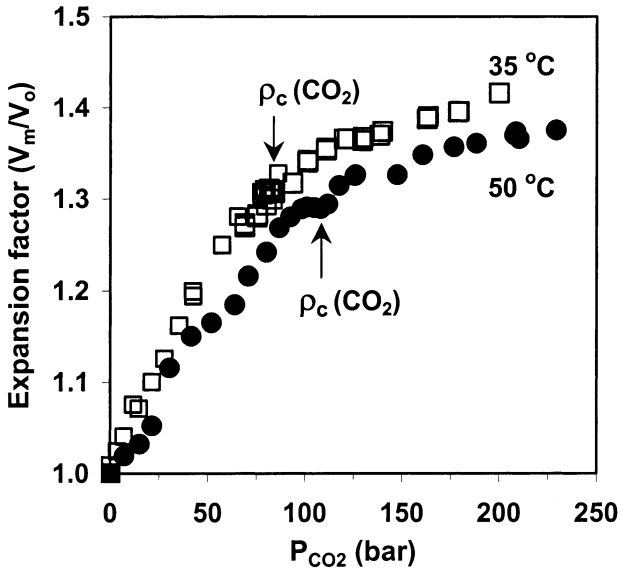


**Figure 2.** Expansion factor of [bmim][$PF_6$] due to added $CO_2$ as a function of $CO_2$ pressure.

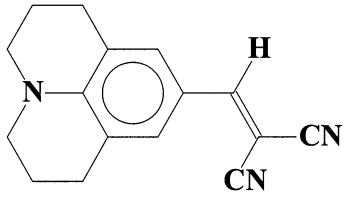


**Figure 3.** Chemical structure of DCVJ.

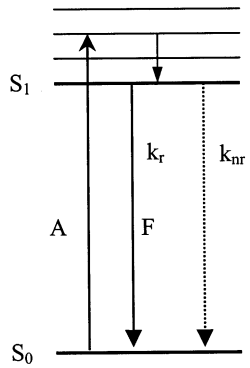


**Figure 4.** Fluorescence emission mechanism. $S_0$, ground state; $S_1$, first excited state; A, absorbance process; F, fluorescence emission process.

2-fold photophysical phenomena related to solvent effects: a microviscosity-dependent fluorescence intensity and a polarity-dependent emission maximum.[32−35]

*Microviscosity.* The fluorescence emission mechanism for DCVJ is illustrated in Figure 4. The fluorescence quantum yield ($\phi_f$) is expressed as

$$\phi_f = k_r/(k_r + k_{nr}) \quad (2)$$

where $k_r$ and $k_{nr}$ are the radiative rate and the nonradiative deactivation rate, respectively. The nonradiative deactivation of the singlet excited state can occur rapidly through intramolecular torsional relaxation about the donor−acceptor bond. An increase in rigidity and viscosity of the surrounding medium tends to inhibit the internal molecular rotation, and as a consequence, the radiative decay rate ($k_r$) becomes dominant. The resultant fluorescence quantum yield is enhanced in such a highly constrained microenvironment (i.e., high microviscosity).

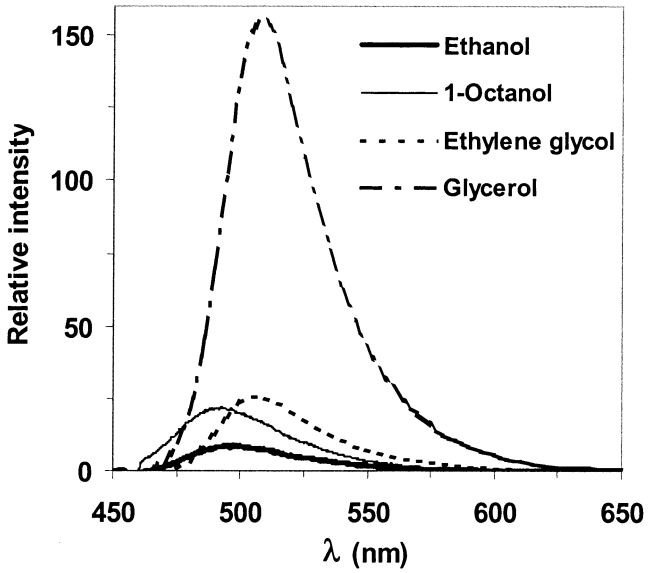


**Figure 5.** Fluorescence emission spectra of DCVJ in conventional liquid solvents at 25 °C ($C_{DCVJ} = 4.5 \times 10^{-6}$ mol/L).

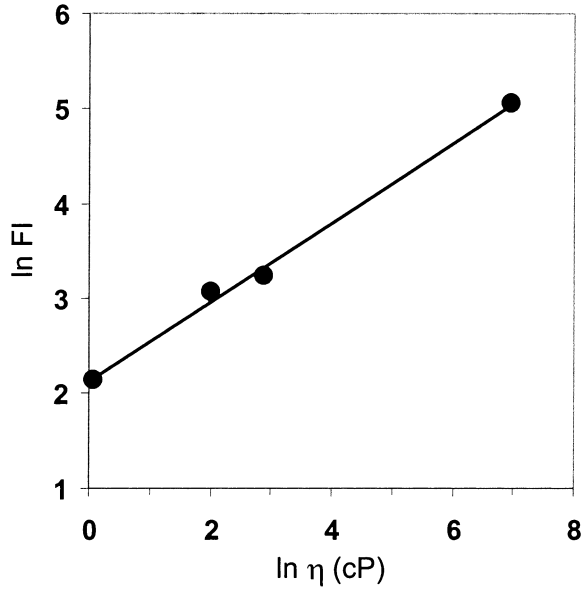


**Figure 6.** Viscosity dependence of fluorescence intensity of DCVJ for the liquid solvents in Figure 5.

Fluorescence spectra of DCVJ were measured in a series of conventional liquids spanning a broad range of viscosity as references for correlation. All spectra in the liquids taken at 25 °C are shown in Figure 5 with peaks in the range of 480−510 nm due to the $\pi \rightarrow \pi^*$ charge-transfer transition of DCVJ. We assume that negligible heterogeneity on a molecular scale exists in these incompressible liquids, so that microviscosity is equivalent to the bulk viscosity. Figure 6 shows an excellent correlation between the relative fluorescence intensity (FI) of DCVJ and the viscosity ($\eta$) of these solvents. The fluorescence spectral measurements were conducted for [bmim][$PF_6$]/$CO_2$ in the pressure range of 0−205 bar and at 35 °C. With the addition of $CO_2$, the concentration of the fluorophore decreases because of volume expansion. The fluorescence spectra were corrected by multiplying the expansion factor under corresponding conditions to ensure that all of the intensities were evaluated for the same concentration of the probe. Figure 7 shows several representative spectra, which reveal that the fluorescence intensity decreases remarkably with increasing $CO_2$ pressure.

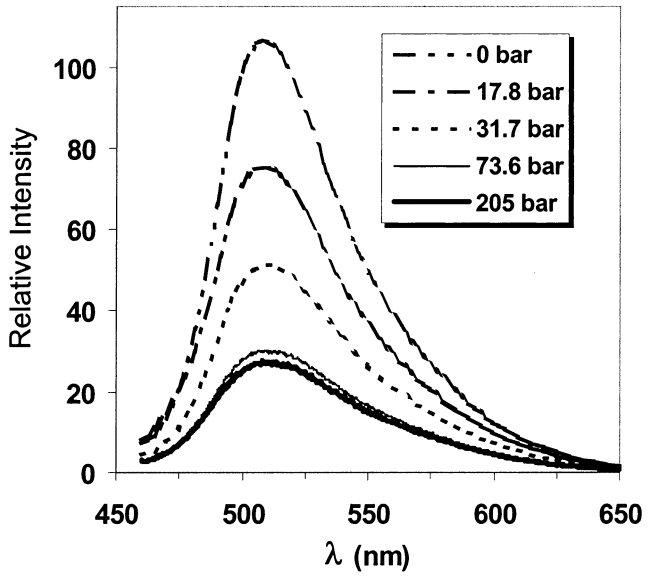


**Figure 7.** Corrrected fluorescence spectra of DCVJ by volume expansion in [bmim][$PF_6$]/$CO_2$ at different pressures and 35 °C ($C_{DCVJ} = 4.5 \times 10^{-6}$ mol/L).

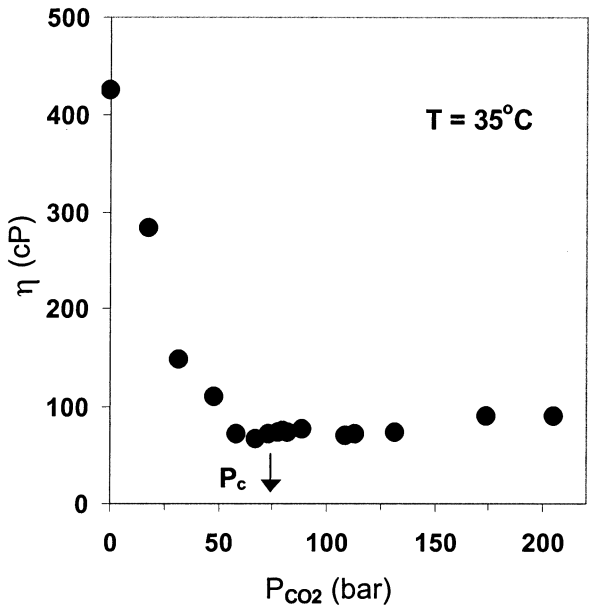


**Figure 8.** Estimated microviscosity for [bmim][$PF_6$]/$CO_2$ as a function of pressure of $CO_2$ at 35 °C.

We applied a linear relationship of ln FI ∝ ln $\eta$ correlated in Figure 6 and estimated the microviscosity in the immediate environment of the probe from the measured fluorescence intensities in [bmim][$PF_6$]/$CO_2$. The results depicted in Figure 8, where the arrow refers to the critical pressure ($P_c$) of $CO_2$, show that the microviscosity of [bmim][$PF_6$] is reduced significantly in the presence of $CO_2$. There appears to be a maximum reduction when $CO_2$ in the vapor phase is in the near-critical region. The local viscosity decreases from 425 to 65 cP as the pressure increases from 0 to 68 bar at 35 °C. The phenomenon is in agreement with the work of Baker et al., who reported about a 5-fold reduction in viscosity,[23] although their estimated viscosity for neat [bmim][$PF_6$] is lower than our results and other published data.[10] It has been recognized, however, that small amounts of impurities in an ionic liquid can cause a variation in viscosity.[10] Additionally, the rapid decline in microviscosity at lower pressures is followed by a slight increase as the $CO_2$ pressure continues to increase. The profile is

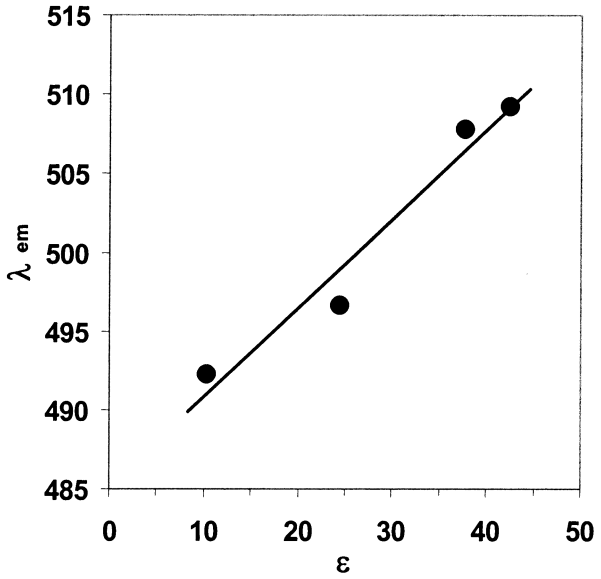


**Figure 9.** Correlation of fluorescence emission maximum of DCVJ with dielectric constant for the ambient liquid solvents at 25 °C.

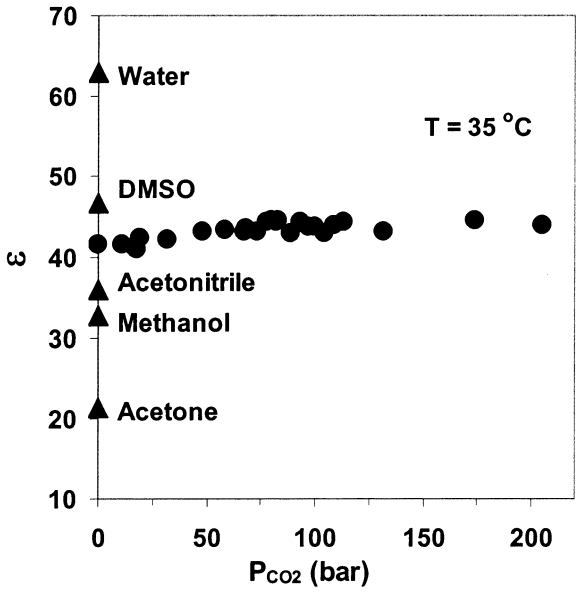


**Figure 10.** Estimated dielectric constants for [bmim][$PF_6$]/$CO_2$ as a function of pressure of $CO_2$ at 35 °C.

consistent with that of the expansion factor, where the maximum expansion occurs around the critical pressure of $CO_2$. The added $CO_2$ appears to have the capability of "lubricating" the viscous RTIL even at moderate pressures, which could dramatically minimize transport resistance and facilitate separation in RTIL/$CO_2$ mixtures.

*Local Dielectric Property.* Because the $\pi^*$ excited-state for DCVJ contains a considerable amount of charge-transfer character, the excited state and the ground state have substantially different dipole moments ($\mu_e \approx 24$ D, $\mu_g \approx 9$ D).[35] As a result, the fluorescence emission maximum is strongly dependent on the polarity of the solvent, which allows the microscopic dielectric property to be probed in the vicinity of the fluorophore molecule. It is evident from Figure 5 that the emission maximum ($\lambda_{em}$) shifts to longer wavelength with an increase in the solvent polarity. The correlation of $\lambda_{em}$ and the dielectric constant ($\epsilon$) of the corresponding solvent (Figure 9) shows a satisfactory linear relationship, from which the dielectric constant of [bmim][$PF_6$]/$CO_2$ at different pressures and 35 °C was calculated. The results shown in Figure 10 demonstrate that the local dielectric constant in the immediate surroundings of the probe is independent of the $CO_2$ solubility. The dielectric constant is estimated to range between 41 and 44, given experimental uncertainty. The general shape of the local dielectric constant for [bmim][$PF_6$]/$CO_2$ estimated from fluorescence spectroscopy is consistent with the Kamlet−Taft $\pi^*$ parameters. Both methods show that the polarity of [bmim][$PF_6$]/$CO_2$ is slightly weaker than those of water and DMSO, but stronger than those of acetone and methanol.

## Conclusions

We utilized two spectroscopic techniques to explore the influence of dissolved $CO_2$ on the microscopic solvent properties of [bmim][$PF_6$] at different temperatures and pressures. Solvatochromism of *N*,*N*-dimethyl-4-nitroaniline was used to measure the Kamlet−Taft solvent parameter $\pi^*$ and the volume expansion of [bmim][$PF_6$]/$CO_2$ mixtures. We see that the dipolarity/polarizability of [bmim][$PF_6$] undergoes minimal reduction at a constant temperature in the presence of $CO_2$ over a wide pressure range; the volume expansion of [bmim][$PF_6$]/$CO_2$, however, increases significantly to about the critical density of $CO_2$. Fluorescence emission spectra of DCVJ probe the microviscosity and the local dielectric constant of [bmim][$PF_6$]/$CO_2$ around the probe on the basis of the correlation of fluorescence quantities with physical properties for known solvents. The polarity in terms of local dielectric constant is independent of the $CO_2$ solubility. The $\pi^*$ parameter and local dielectric constant both indicate that the polarity of [bmim][$PF_6$] with and without $CO_2$ is slightly lower than those of DMSO and water, but noticeably higher than those of acetonitrile, acetone, and methanol. On the other hand, the microviscosity of [bmim][$PF_6$]/$CO_2$ in the immediate surroundings of DCVJ is reduced by a factor of 6.5 as the pressure of added $CO_2$ increases from 0 to 68 bar at 35 °C and subsequently undergoes a small increase up to 203 bar. Possibly, the addition of $CO_2$ bears little impact on the change in the polarity of [bmim][$PF_6$] due to a preferential solvation effect of the RTIL with a polar solute, yet it results in a dramatically reduced microviscosity in the vicinity of the probe molecule. The effect of added $CO_2$ on the microviscosity might be significant for promoting mass transport and facilitating separation for normally viscous RTILs.

**Acknowledgment.** The authors are grateful for help from Dr. James Brown and Karl Counts for construction of the spectroscopic cell used in this work. We also thank Nina Paolella for her laboratory assistance with the fluorescence spectral measurements.

## References and Notes

(1) Wasserscheid, P.; Welton, T. *Ionic Liquids in Synthesis*; Wiley-VCH: Weinheim, Germany, 2002.
(2) Welton, T. *Chem. Rev.* **1999**, *99*, 2071.
(3) Gordon, C. M. *Appl. Catal. A* **2001**, *222*, 101.
(4) Olivier-Bourbigou, H.; Magna, L. *J. Mol. Catal.* **2002**, *3484*, 1.
(5) Cull, S. G.; Holbrey, J. D.; Vargas-Mora, V.; Seddon, K. R.; Lye, G. J. *Biotechnol. Bioeng.* **2000**, *69*, 227.
(6) Nara, S. J.; Harjani, J. R.; Salunkhe, M. M. *Tetrahedron Lett.* **2002**, *43*, 2979.
(7) Hyk, W.; Stojek, Z. *J. Phys. Chem. B* **1998**, *102*, 577.
(8) Scurto, A.; Aki, S.; Brennecke, J. *J. Am. Chem. Soc.* **2002**, *124*, 10276.
(9) Ngo, H. L.; LeCompte, K.; Hargens, L.; McEwen, A. B. *Thermochim. Acta* **2000**, *357*, 97.
(10) Huddleston, J. G.; Visser, A. E.; Reichert, W. M.; Willauer, H. D.; Broker, G. A.; Rogers, R. D. *Green Chem.* **2001**, *3*, 156.
(11) Eckert, C. A.; Knutson, B. L.; Debenedetti, P. G. *Nature* **1996**, *383*, 313.
(12) Blanchard, L. A.; Gu, Z.; Brennecke, J. F. *J. Phys. Chem. B* **2001**, *105*, 2437.

(13) Blanchard, L. A.; Hancu, D.; Beckman, E. J.; Brennecke, J. F. *Nature* **1999**, *399*, 28.
(14) Brennecke, J. F.; Maginn, E. J. *AIChE J.* **2001**, *47*, 2384.
(15) Hou, Z.; Han, B.; Gao, L.; Jiang, T.; Liu, Z.; Chang, Y.; Zhang, X.; He, J. *New J. Chem.* **2002**, *26*, 1246.
(16) Brown, R. A.; Pollett, P.; McKoon, E.; Eckert, C. A.; Liotta, C. L.; Jessop, P. G. *J. Am. Chem. Soc.* **2001**, *123*, 1254.
(17) Liu, F.; Abrams, M. B.; Baker, R. T.; Tumas, W. *Chem. Commun.* **2001**, 433.
(18) Lozano, P.; deDiego, T.; Carrie, D.; Vaultier, M.; Iborra, J. L. *Chem. Commun.* **2002**, 692.
(19) Peng, J.; Deng, Y. *New J. Chem.* **2001**, *25*, 639.
(20) Bösmann, A.; Franciò, G.; Janssen, E.; Solinas, M.; Leitner, W.; Wasserscheid, P. *Angew. Chem.* **2001**, *113*, 2769.
(21) Blanchard, L. A.; Brennecke, J. F. *Ind. Eng. Chem. Res.* **2001**, *40*, 287.
(22) Sellin, M. F.; Webb, P. B.; Cole-Hamilton, D. J. *Chem. Commun.* **2001**, 781.
(23) Baker, S. N.; Baker, G. A.; Kane, M. A.; Bright, F. V. *J. Phys. Chem. B* **2001**, *105*, 9663.
(24) Kazarian, S. G.; Briscoe, B. J.; Welton, T. *Chem. Commun.* **2000**, 2047.
(25) Ely, J. F.; Haynes, W. M.; Bain, B. C. *J. Chem. Thermodyn.* **1989**, *21*, 879.
(26) Kamlet, M. J.; Abbound, J. L. M.; Taft, R. W. *J. Am. Chem. Soc.* **1977**, *99*, 6027.
(27) Baker, S. N.; Baker, G. A.; Bright, F. V. *Green Chem.* **2002**, *4*, 165.
(28) Marcus, Y. *Chem. Soc. Rev.* **1993**, 409.
(29) Carmicheal, A. J.; Seddon, K. R. *J. Phys. Org. Chem.* **2000**, *13*, 591.
(30) Aki, S. N. V. K.; Brennecke, J. F.; Samanta, A. *Chem. Commun.* **2001**, 413.
(31) Muldoon, M. J.; Gordon, C. M.; Dunkin, I. R. *J. Chem. Soc., Perkin Trans.* **2001**, *2*, 433.
(32) Kung, C. E.; Reed, J. K. *Biochemistry* **1986**, *25*, 6114.
(33) Kung, C. E.; Reed, J. K. *Biochemistry* **1989**, *28*, 6678.
(34) Loutfy, R. O.; Arnold, B. A. *J. Phys. Chem.* **1982**, *86*, 4205.
(35) Loutfy, R. O. *Pure Appl. Chem.* **1986**, *58*, 1239.